EXPERIMENTAL VALIDATION OF CROSSTALK SIMULATIONS FOR ON-CHIP INTERCONNECTS AT HIGH FREQUENCIES USING S-PARAMETERS

Mauro J. Kobrinsky[1,†], Sourav Chakravarty[2], Dan Jiao[3], Michael Harmes[1], Scott List[1] and Mohiuddin Mazumder[3]

[1]Components Research, Logic Technology Development, Intel Corporation, RA3-252, 2513 NW 229th, Hillsboro, OR 97124; [2]TCAD, Logic Technology Development, Intel Corporation, RA3-254, 2513 NW 229th, Hillsboro, OR 97124; [3]TCAD, Logic Technology Development, Intel Corporation, SC12-205, 3600 Juliette Ln, Santa Clara, CA 95064.

ABSTRACT

Since advanced microprocessors are designed based on simulation tools, accurate assessments of the amount of crosstalk noise are of paramount importance to avoid logic failures and less-than-optimal designs. With increasing clock frequencies, inductive effects become more important, and the validity of assumptions commonly used in simulation tools and approaches is unclear. We compared accurate experimental S-parameters with results derived from both magneto-quasi-static and full-wave simulation tools, for simple crosstalk structures with various capacitive and inductive couplings, in the presence of parallel and orthogonal conductors. Our validation approach made possible the identification of the strengths and weaknesses of both tools as a function of frequency, which provides useful guidance to designers who have to balance the trade-offs between accuracy and computation expenses for a large variety of cases.

Keywords: validation, signal integrity, S-parameters.

INTRODUCTION

Present advanced microprocessor designs rely heavily on simulation results, since time and resource constraints make impossible the experimental assessment of all cases of interest. Inaccuracies in the estimated crosstalk noise could result in logic failures and less-than-optimal designs. Furthermore, the uncertainties associated with simulation tools that have not been validated typically translate into conservative non-optimal designs. Unfortunately, obtaining the high-quality experimental data at high frequencies (tens of GHz) that is needed to validate simulation tools is challenging because of parasitics that can significantly distort the experimental results.

A complete experimental validation using structures implemented in a full flow Si testchip with drivers and receivers can potentially provide realistic results to investigate signal integrity, but it would require significant layout time and manufacturing expenses, and is usually not a practical option. In addition, active Si measurements of crosstalk noise are typically indirect and benefit greatly when combined with passive measurements. On the other hand, the relatively low cost of passive-structure testchips (i.e. with no active Si devices) provides the opportunity for fabricating and testing hundreds of test structures, which facilitates the identification of the underlying physical mechanisms that govern signal integrity.

In this paper, we investigate the behavior of simple passive crosstalk structures in which we varied key physical dimensions (e.g. spacings and lengths), as well as the orientation of the conductors in the layers above and below the signal lines, to obtain different levels of inductive and capacitive couplings. The experimental characterization of the test structures was carried out by measuring their S-parameters, from which we removed the parasitics using a de-embedding approach that we developed. In addition, we used a quasi-magneto-static and a full-wave simulation tools to calculate the behavior of the test structures, which we compared to the experimental results to identify their strengths and weaknesses.

EXPERIMENTAL

We considered passive test structures fabricated using three levels of metal, to which we will refer as M1, M2, and M3 (Fig. 1a). The structures basically consisted of two parallel signal lines in M2, wide solid returns in M2, and additional returns of two different type in M1 and M3. One of the signal lines in M2 was 1 μm wide while the other was 2 μm wide. Structures E1 (E11, E12, E13, E14) have 50 % dense conductors in M1 and M3 (i.e. the Cu conductors occupied 50 % of the total area), formed by 1 μm-wide lines running perpendicular to the M2 signal lines. Structures E22 have 50 % dense returns in M1 and M3 composed of 1 μm-wide lines running parallel to the signal lines. By varying the distance between the signal lines (*s2*) and the distance between signal lines and returns in M2 (*g2*), different levels of capacitive and inductive couplings were obtained. Table 1 summarizes the dimensions of the crosstalk structures, which were measured using high resolution SEM cross sections and optical microscopy. A single value of line length (2 mm) is considered for the E1 structures, and two different line lengths are used for E22 (2 and 8 mm). The dc resistivity of the Cu lines was obtained by measuring the total resistance of lines of different lengths, and was found to be 1.97 μΩ-cm. The effective dielectric constant of the combined Si and Si nitride layers was measured at 1 MHz. For both M2 signal lines, one of the ends was left open, while the other was connected to a bondpad, resulting in two-port structures (see Fig. 2a). Since the bondpads were both on the same side of the lines, the measurements corresponded to the so-called near end crosstalk noise.

† *Corresponding author: email: mauro.j.Kobrinsky@intel.com, phone: 971-214-5645, fax: 971-214-7805.*

The electrical behavior of the structures was experimentally characterized by measuring their S-parameters in the frequency range 45 MHz-40 GHz, using an HP8510 system. The dimensions of the bondpads were 50 x 35 μm^2, which were probed with 50 µm-pitch ground-signal-ground microwave probes.

The S-parameters, S_{ij}, of two port structures form a matrix of rank 2: S_{11} is the reflection at port 1, while S_{12} represents the crosstalk between ports 1 and 2. Two important advantages of S-parameters are that: (1) they can be accurately measured, and (2) they allow de-embedding of parasitics (will be discussed later). In addition, they also provide a direct measure of the amount of crosstalk at *each* frequency (S_{12}), which is of great importance since, as we will show later, the amount of crosstalk strongly depends on frequency in a non-monotonic manner, and can increase or decrease with increasing frequency. Finally, it is important to mention that, given the S-parameters and the reference impedance (50 Ω in this work), the time-domain response can be calculated for any excitation and loading condition. On the contrary, a given time-domain result (i.e. voltage-time) is only valid for the particular rise time, pulse shape, and termination conditions of the experiment.

Table 1: structures considered in this report.

	E11	E12	E13	E14	E22
s2	0.19 µm	0.18 µm	1.98 µm	1.95 µm	2.0 µm
g2	1.0 µm	10.2 µm	0.98 µm	10.3 µm	10.7 µm
M1 and M3 conductors	perpendicular	perpendicular	perpendicular	perpendicular	parallel

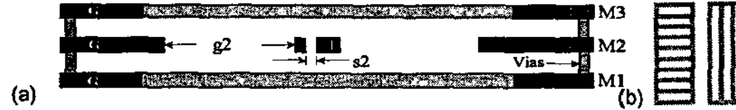

Figure 1. (a) Cross sectional view of the crosstalk structures, indicating the definition of *s2* and *g2*. Line widths are 1 and 2 µm. (b) Top view of the two types of returns in M1 and M3 considered in this paper.

To measure the response of the signal lines, cables, probes, bondpads, access lines and vias are necessary (Fig. 2a). Unfortunately, these additional elements also contribute to the measured S_{ij}, in a complicated frequency-dependent manner. The removal of these undesirable signals, referred to as parasitics, is a difficult task that has hindered many previous validation attempts. The parasitics introduced by the cables and the probes were removed following the well-known SOLT technique [1] using a calibration substrate (i.e. off die). To remove the remaining parasitics generated by the bondpads, vias, and access lines, we developed a de-embedding technique that builds upon the YZ-matrix technique, and that allowed us to accurately remove the parasitics. We modeled the parasitics with general frequency-dependent Z and Y elements (Fig. 2b.), which are unknown.

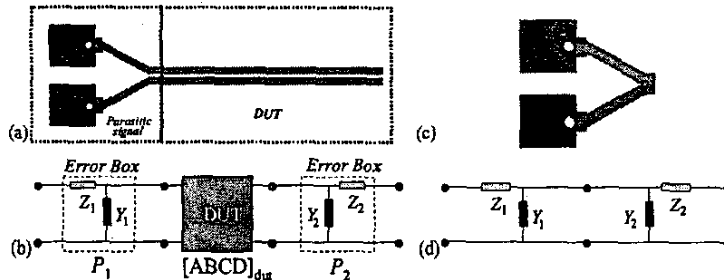

Figure 2. (a) Schematics of the structures. (b) Circuit model, showing the parasitics sources and the DUT. (c) Schematics of a "Thru" calibration structure. (d) Circuit model for the "Thru".

Mathematically, it is convenient to use [ABCD] matrices, which allow cascading of elements in series [1]. If the Y and Z parameters are given, the ABCD matrix of the DUT can be obtained using:

$$\begin{pmatrix} a & b \\ c & d \end{pmatrix}_{DUT} = \begin{pmatrix} 1+Y_1Z_1 & Z_1 \\ Y_1 & 1 \end{pmatrix}^{-1} \cdot \begin{pmatrix} a & b \\ c & d \end{pmatrix}_{meas} \cdot \begin{pmatrix} 1 & Z_2 \\ Y_2 & 1+Y_2Z_2 \end{pmatrix}^{-1} \qquad (1)$$

where $(\{a, b\},\{c, d\})_{meas}$ is the (known) [ABCD] matrix obtained from the measured S_{ij}, $(\{a, b\},\{c, d\})_{DUT}$ is the (unknown) [ABCD] matrix of the DUT, the other two matrices are the [ABCD] matrices of the two error boxes shown in Fig. 2b (P_1 and P_2), and Y_i and Z_i (with i = 1, 2) are the parameters used to describe each parasitic box. To obtain these parameters, we used "Thru", "Short" and "Open" calibration structures (Fig. 2c shows a "Thru"). For example, for a Thru calibration structure, the following equation can be written:

$$\begin{pmatrix} a & b \\ c & d \end{pmatrix}_{THRU} = \begin{pmatrix} 1+Y_1Z_1 & Z_1 \\ Y_1 & 1 \end{pmatrix} \cdot \begin{pmatrix} 1 & Z_2 \\ Y_2 & 1+Y_2Z_2 \end{pmatrix} \quad (2)$$

Similar equations can be written for the other two types of calibration structures. We measured the S-parameters of Thru, Open and Short calibration structures, from which we obtained (Y_i, Z_i) for each port as a function of frequency, using Eq. 2 and the analogous equations for the Short and Open calibration structures. A more detailed description of the estimation of de-embedding errors, which were found to be below 10 %, will be presented elsewhere.

SIMULATIONS

Simulation results derived with two different simulation tools are presented in this paper: a 2D magneto-quasi-static tool, and a full-wave tool. The magneto-quasi-static tool uses a PEEC (partial element equivalent circuit) formulation for R and L extraction, and a pure static formulation for the C extraction, where R, L, and C are, respectively, the resistance, inductance and capacitance per unit length of interconnect. In this tool, the conductors in M2 were modeled as lossy transmission lines for all structures. For structure E22, the conductors in M1 and M3 were also modeled as transmission lines. For structures E11-E14, which have perpendicular conductors in M1 and M3, the capacitances was extracted by replacing the perpendicular conductors by a solid metal plane, but they were removed for the R and L extractions. The Si substrate was modeled as a conductor.

The full-wave solver is a rigorous Maxwell's partial differential equation solver for modeling of waveguiding structures recently developed at Intel. This tool represents the original wave propagation problem into a generalized eigen-value problem. The resulting eigen-value representation can accurately comprehend both conductor and dielectric losses, arbitrary conductor and dielectric configurations, and arbitrary materials. The propagation characteristics along the longitudinal direction are explicitly introduced to rigorously reduce the discretization of 3D spaces to the transverse cross section only, which significantly reduces the computational complexity. A mode-matching technique applicable to lossy system is developed to solve large-scale 3D problems by using 2D-like CPU time and memory. For structures E11-E14, unlike the 2D magneto-quasi-static tool, all perpendicular conductors in M1 and M3 are rigorously modeled. A more detailed description can be found in [2].

RESULTS AND DISCUSSION

Figure 3 compares the magnitude of S_{12} obtained with the magneto-quasi-static and the full-wave tools, to the de-embedded experimental results, as a function of frequency. From Fig. 3, the following conclusions can be made:

1. There is an excellent agreement between both simulation tools and experiments for structures with parallel conductors in M1 and M3.
2. There is a significant frequency shift, in the range of 2-7 GHz, between the magneto-quasi-static simulations and the experiments for structures with perpendicular conductors in M1 and M3. On the contrary, an excellent agreement is observed between the full-wave results and the experiments.
3. The crosstalk noise level is an order of magnitude larger in the presence of perpendicular interconnects than in the presence of parallel interconnects in M1 and M3.

The very good agreement between the magneto-quasi-static tool and experiments at tens of GHz is suggesting that the magneto-static approximation holds for structures with parallel returns in the frequency range of interest in this paper. For the structures with perpendicular conductors in M1 and M3, only the full-wave tool accurately captures the experimental data, while the magneto-quasi-static results are affected by a significant frequency shift. It is relevant to mention that frequency shifts translate to delays in the time domain. It is also interesting to note that the frequency shift becomes significant at frequencies above 10 GHz, which as a rule of thumb, corresponds to 1-3 GHz digital signals. Consequently, for present and future clock speeds, an improper characterization of structures with perpendicular conductors could have adverse implications on timing, clock and signal integrity assessments. In addition, Fig. 3 shows that the amount of crosstalk strongly depends on frequency in a non-monotonic manner, and suggests that special care should be taken when performing analysis of crosstalk at a single frequency. It is interesting to note that the values of S_{12} of E22 are an order of magnitude smaller than those of structures E1, which is expected since the parallel conductors in M1 and M3 of E22 are more efficient current return paths than the perpendicular conductors in M1 and M3 of structures E1. Finally, the magnitude of the disagreement between the static results and experimental data was found to be significant for all the E1 structures, which have different relative inductive and capacitive coupling strengths. A possible cause of the observed discrepancies between the static simulations and the experiments could

be partially due to the 3D nature of the structure at hand, but dominantly due to the decoupled model of E and H used in the magneto-quasi-static tools.

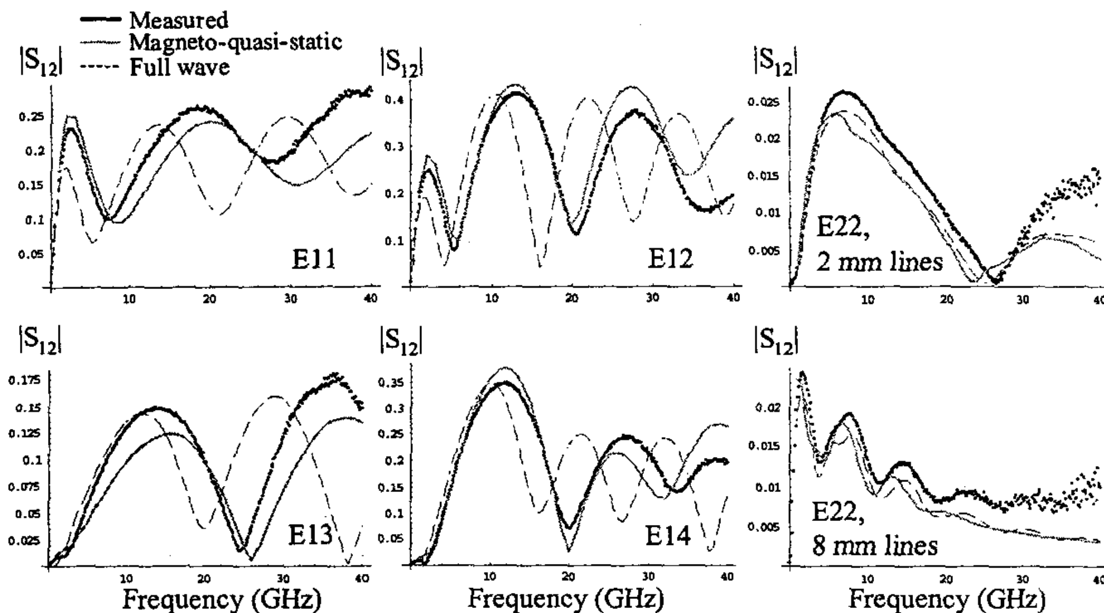

Figure 3. Measured $|S_{12}|$ as a function of frequency for structures with perpendicular conductors in M1 and M3 (E11, E12, E13 and E14) and for structures with parallel conductors in M1 and M3 (E22).

SUMMARY AND CONCLUSIONS

We described an experimental approach that provides accurate high frequency S-parameters, which enabled us to identify the strengths and limitations of two simulation tools that represent two common cases in this field: a 2D magneto-quasi-static and a 3D full-wave tool. *We found that both type of simulators can accurately capture the response of structures with parallel* conductors. On the contrary, in the presence of relevant conductors that run perpendicular to signal lines, only the full-wave *tool provided accurate results.* The observed discrepancies between the static simulations and the experiments was ascribed to the 3D nature of the structure at hand and to the decoupled model of E and H used in the magneto-quasi-static tools.

Our validation approach made possible the identification of the strengths and weaknesses of both approaches as a function of frequency, which provides useful guidance to designers that have to balance the trade-offs between accuracy and computation expenses for a large variety of practical situations.

ACKNOWLEDGMENTS

The authors wish to acknowledge Dr. E. Chiprout and W. Pinello for valuable discussions.

BIBLIOGRAPHY/REFERENCES

[1] D. M. Pozar, Microwave Engineering, 2nd ed., John Wiley & Sons, 1998.

[2] D. Jiao, M. Mazumder, S. Chakravarty, C. Dai, M. Kobrinsky, M. Harmes, and S. List, "A novel technique for full-wave modeling of large-scale three-dimensional high-speed on/off-chip interconnect structures", SISPAD 2003.